Force Field Development for Poly(dimethylsilylenemethylene) with the Aid of ab Initio Calculations

Vasilios E. Raptis and Vasilios S. Melissas*

Department of Chemistry, University of Ioannina, GR-451 10 Ioannina, Greece

Received: October 11, 2005; In Final Form: June 2, 2006

The molecular geometries, conformational energies, and zero-point energies of di(trimethylsilylene)methylene have been determined from high-level quantum chemistry calculations. The results are further used in the parametrization of a classical potential energy function suitable for performing simulations of the corresponding polymer, namely, poly(dimethylsilylenemethylene). Di(trimethylsilylene)methylene geometrical parameter optimizations for a proper location of the global minimum and other local minima, constrained at certain dihedral and bond angles, were performed at both the B3LYP/6-311G and MP2(full)/6-311G levels of theory. The global minimum configuration is slightly displaced from a perfectly staggered geometry, approximately by 16.0°, at both levels of theory. Molecular mechanics and Monte Carlo calculations for isolated polymer chains together with molecular dynamics runs for the modeled dimer provide very good results in terms of conformational and thermodynamic properties.

I. Introduction

Poly(dimethylsilylenemethylene), PDMSM, is an organosilicon analogue of poly(dimethylsiloxane), PDMSO, which could be formally derived by the latter through the oxygen main chain atom replacement by methylene groups. PDMSO, a highly flexible polymer with the lowest known glass transition temperature, and its derivatives offer rubbery amorphous materials with widespread use in industrial and everyday applications.[1] Its utilization as a gas separation membrane by the natural gas and petroleum associated gas industry has emerged in the last 15 years, mostly at a pilot plant level.[2] Its attractive permeance properties are mainly based on the high solubility of the heavy compounds found in raw hydrocarbon mixtures. However, sulfur containing compounds such as H_2S and mercaptane, which are present in some of the above mixtures, are capable of attacking the polymer Si−O bond, through hydrolysis reactions,[3] thus destroying the membrane structure and eliminating its permeance properties. One way to surmount the problem would be the PDMSO membrane replacement by a material combining equally good permeation with resistance to chemically harmful environments. PDMSM is one such material, due to (i) its structural similarity to PDMSO and (ii) the existence of the chemically resistant Si−C bond instead of the vulnerable Si−O one.

PDMSM comprises the simplest representative of a large family of organosilicon polymers, where all members have a $-[SiR_AR_B-C_m]_n-$ type of structure in common, with $m = 1$, 2, 3 and R_A and R_B being aliphatic, aromatic, or even more complex groups. A thorough study of a number of these polymers has recently been completed,[4−6] combining experimental techniques with equations of state and, especially for PDMSM, molecular dynamics, MD, simulation. Results have shown that polymers such as PDMSM, poly(dimethylsilylenetrimethylene), PDMSTM, and the copolymer PDMSM-*co*-PDMSTM offer promising alternatives to PDMSO membranes. Since no previous attempts to simulate organosilicon polymers, beyond PDMSO, were known, the simulations relied upon a newly developed force field. The original force field version used in that study was devised through a combination of (i) extensive B3LYP/6-311G[8] quantum mechanical calculations and (ii) fitting to known thermodynamic data related to the monomer and dimer of PDMSM. Use of the new model yielded very good agreement between calculated and experimental thermodynamic data for the pure polymer and for its mixtures with normal alkanes, and acceptable agreement between calculated diffusivities and available experimental permeance data. The force field implementation focused on reproduction of the bulk polymer properties, rather than depicting the detailed conformational behavior of isolated molecules.

The united atom representation was adopted throughout that study; that is, methyl and methylene groups were represented as single interaction sites. The parameters used were divided into two classes: (i) the "nonlocal" one, comprising only Lennard-Jones potential parameters, and (ii) the "local" one consisting of all bonded terms plus an additional set of Lennard-Jones parameters for atoms belonging to the same molecule but separated by three or four bonds. This is a flexible, highly modular scheme capable of coping with many polymers of the type considered here, without further need to reevaluate parameters for a specific element−interaction site, bond, angle, torsion angle−once they are determined (assumption of transferability). Moreover, the distinction between nonlocal and local terms allows for individual refinement of each parameter class, for the purpose of reliably predicting thermodynamic (nonlocal dependent) or conformational (local dependent) properties, respectively.[9,10] Local parameters were derived by appropriate fitting to quantum mechanical results for di(trimethylsilylene)-methylene, DTMSM, the fundamental dimer of PDMSM, Figure 1a, whereas nonlocal ones relied upon monomer and dimer thermodynamic data.

The initial model version predicted a dimer minimum energy configuration, where the two main C−Si−C−Si dihedral angles exhibited a trans symmetry, namely, 180.0°, in accordance with

* Corresponding author. Phone: +3026-5109-8471. Fax: +3026-5109-8682. E-mail: melissas@chem.auth.gr.

10.1021/jp055798t CCC: $33.50
Published on Web 07/13/2006

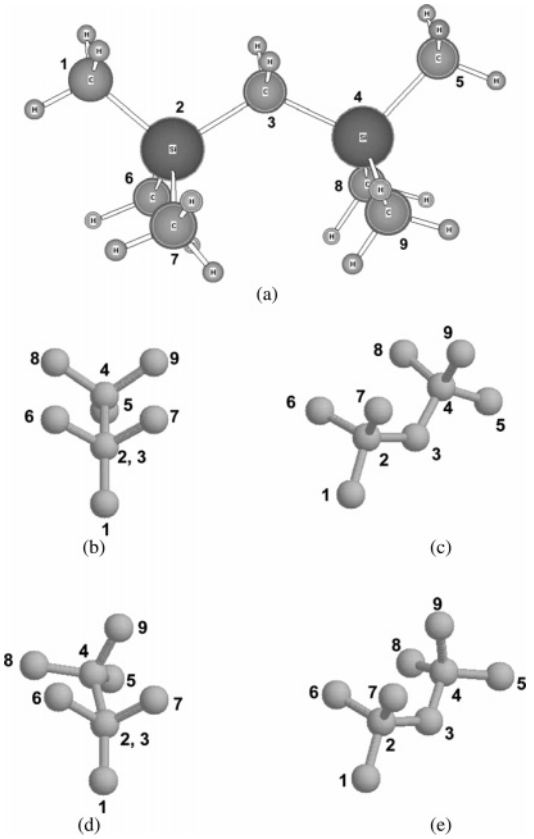

Figure 1. The DTMSM molecule. An explicit atom representation is shown in part a. Heavy atoms (Si, C) are numbered from 1 through 9. The united atom representation is shown as an all trans conformation, Newmann projection, part b, all trans conformation, side view, part c, minimum energy conformation, Newmann projection, part d, and minimum energy conformation, side view, part e.

the quantum mechanical results, as depicted in Figure 1b and c. However, vibrational frequency analysis resulted in a very low imaginary frequency, which triggered the suspicion that the all trans conformer represents a remarkably flat saddle point rather than a minimum. Indeed, second-order Møller−Plesset[11] perturbation calculations, exempt of any symmetry constraints, revealed the existence of a global minimum with both previous dihedral angles equal to about 164.0° positioned crosswise, as shown in Figure 1d and e, and an energy difference from the all trans saddle point equal to 0.49 kcal mol^{-1}. A similar calculation for the global minimum followed at the B3LYP[8] level of theory, which confirmed the newly found topology of the potential energy hypersurface. Symmetry considerations suggest the existence of two such equidistant minima on both sides of a trans point. This is reminiscent of the split potential well existent in poly(isobutylene),[12] as well as poly(dimethylsilane),[13] and is apparently due to the existence of the methyl groups attached to the backbone atoms.

Although thermodynamic properties are not expected to be directly affected by this defect of the original model, the conformational behavior of the simulated polymer might suffer significant changes. PDMSO and PDMSM carry a common main chain sequence of successively alternating Si−X−Si and X−Si−X angles with different average values, where X denotes O and C, respectively. This kind of structure results in a closed loop form of the all trans conformation of long polymer chains.[14] However, if all main dihedral angles exhibit a certain deviation from the all trans configuration, spiral elongated conformations would be adopted by the macromolecular chains. The system's ability to explore an extensive potential valley with two "dislocated" shallow minima, rather than being confined in a narrow potential well of the trans conformation, is expected to result in non-negligible differences regarding frequent access to expanded conformations. This should, in turn, affect such properties as shape and size distribution of free volume and eventually gas transport properties of the material. In this respect, revision of the local part of the model was desired, to render it capable of reproducing essential features of the quantum mechanical potential energy hypersurface.

The article structure is organized as follows: In section II, the model employed in the simulations is briefly presented, the quantum mechanics methodology is exposed, and their results are summarized and discussed. In section III, the fitting procedure to the quantum mechanical results is explained and the devised parameters are presented. In section IV, results of validation calculations are given, which confirm the model's ability to provide reliable results. A discussion, conclusions, and future goals of our research are given in section V.

II. The Model and Quantum Mechanical Calculations

Thanks to the development of improved computational methods and the enhancement of computer capabilities, use of ab initio calculations, as a means to create novel force fields, has become an established methodology. Atomistic models have been constructed, not only for small or medium size molecules[15−17] but also for polymers whose respective oligomers have been studied quantum mechanically.[18]

Due to the broad spectrum of polymer dynamics time scales, extending from sub-picoseconds to microseconds or even milliseconds, the simplest possible model is preferably adopted to allow for long enough simulations of sufficiently large systems. A "class I"[15] united atom force field is thereby chosen, where Si, CH_2, and CH_3 consist of the interaction sites comprising the molecule and the potential energy is given by the following expression:

$$V = V_{\text{stretching}} + V_{\text{bending}} + V_{\text{torsion}} + V_{\text{nonbonded}} \qquad (1)$$

where

$$V_{\text{stretching}} = \sum_{i,j} \frac{1}{2} k_{ij}(l_{ij} - l_{ij}^{\circ})^2 \qquad (2)$$

is summed over all bonds connecting united atoms i and j, k_{ij} is the stretching potential constant, l_{ij} is the bond length, and l_{ij}° is the equilibrium bond length

$$V_{\text{bending}} = \sum_{i,j,k} \frac{1}{2} k_{ijk}(\theta_{ijk} - \theta_{ijk}^{\circ})^2 \qquad (3)$$

where the sum runs over the available bond angles formed by united atoms, that is, CH_3−Si−CH_3, CH_2−Si−CH_3, or Si−CH_2−Si, and the quantities involved have a meaning analogous to those of the stretching potential

$$V_{\text{torsion}} = \sum_{i,j,k,l} \frac{1}{2} k_{ijkl}(1 + \cos 3\phi_{ijkl}) \qquad (4)$$

is summed over all torsion—dihedral—angles defined along the polymer main chain, or, in the DTMSM case, over two CH_3−Si−CH_2−Si type angles, k_{ijkl} is an intrinsic potential energy barrier characterizing the torsion of the central bond formed by united atoms j and k, of each dihedral $ijkl$, and

$$V_{\text{nonbonded}} = \sum_{i,j} 4\epsilon_{\text{l},ij}\left(\left(\frac{\sigma_{\text{l},ij}}{r_{ij}}\right)^{12} - \left(\frac{\sigma_{\text{l},ij}}{r_{ij}}\right)^{6}\right) + \sum_{k,l} 4\epsilon_{\text{nl},kl}\left(\left(\frac{\sigma_{\text{nl},kl}}{r_{kl}}\right)^{12} - \left(\frac{\sigma_{\text{nl},kl}}{r_{kl}}\right)^{6}\right) \quad (5)$$

where the local terms, denoted by the subscript "l", encompass interactions among bonded pairs of invoked sites separated by three bonds, namely, 1−4, and intramolecular nonbonded pairs separated by four bonds, namely, 1−5, whereas nonlocal terms, denoted by the subscript "nl", involve all remaining intra- and intermolecular nonbonded pairs, $\epsilon_{\text{l},ij}$ or $\epsilon_{\text{nl},kl}$ denotes the appropriate Lennard-Jones potential energy well, $\sigma_{\text{l},ij}$ or $\sigma_{\text{nl},kl}$ corresponds to the equivalent diameter of the interacting pair, and r_{ij} or r_{kl} is the distance between the invoked sites. In the case of DTMSM, only local terms exist, which comprise two pair types, namely, Si−CH_3 and CH_3−CH_3. The parameters describing pairs that consist of different type sites, α and β, are defined via the well-known Lorentz−Berthelot rules:

$$\sigma_{\alpha\beta} = (\sigma_{\alpha\alpha} + \sigma_{\beta\beta})/2 \quad \text{and} \quad \epsilon_{\alpha\beta} = \sqrt{\epsilon_{\alpha\alpha}\epsilon_{\beta\beta}} \quad (6)$$

Our study is only concerned with local parameters, which can be determined quantum mechanically. Nonlocal Lennard-Jones parameters have been determined via utilization of experimental thermodynamic data and therefore are not considered in this article. Relevant details can be found elsewhere.[4−7] Electrostatic interactions are not accounted for in our model. Interactions of the Coulomb type are mostly used in the following cases: (a) when ionic species are present in the system and (b) as a convenient alternative for the modeling of chemical bond dipole moments by means of partial charges. In the cases of DTMSM and PDMSM, no ions or significant dipole moments exist, and therefore, short range terms, for example, of the Lennard-Jones type, constitute sufficient descriptors of the nonbonded interactions.

DTMSM involves all kinds of local interactions considered here and served as a prototype in the quantum mechanical calculations for the derivation of local parameters. First, the minimum energy configuration was sought, with respect to all degrees of freedom. Then, constrained energy minimization calculations followed for a complete determination of the energy differences between the global minimum geometry and other representative configurations. In those calculations, the two "main" dihedral angles, denoted as φ_1 and φ_2, were fixed at various values. With reference to Figure 1, starting from the all trans configuration, each torsion angle, namely, $CH_3(1)$−Si(2)−$CH_2(3)$−Si(4) and Si(2)−$CH_2(3)$−Si(4)−$CH_3(5)$, was varied in a stepwise manner by 30.0°. Due to the remarkably high symmetry characterizing DTMSM in its united atom representation, 10 (φ_1, φ_2) conformations provide a representative portion of the conformational space defined by fully rotating the two dihedrals.

In the spirit of ref 16, a set of additional constrained calculations were performed, where the main torsion angles were fixed at their trans conformation, and selected bond angles were fixed at values differing by ±1, ±2, and ±3° from their span at the all trans configuration. The all trans conformation was selected as a reference conformation for bond angle calculations in order to decouple the torsion from the rest of the potential energy contributions. Indeed, the torsion energy of bonds connecting two sp^3 hybridized atoms, like Si and C, can be, in general, described by a series[19] of the form

$$V(\phi') = \frac{1}{2}V_3(1 - \cos 3\phi') + \frac{1}{2}V_6(1 - \cos 6\phi') + \ldots = \frac{1}{2}\sum_{n=1}^{\infty} V_{3n}(1 - (-1)^n \cos 3n\phi) \quad (7)$$

where ϕ' denotes dihedral angles in the framework of the convention letting trans be equal to 0.0° and φ corresponds to the convention herein adopted, with the trans conformation assigned a 180.0° value. Therefore, torsion energy proper should be exactly zero at the trans conformation. Besides, the above series is a rapidly converging one; even the V_6 term has been found to be negligible,[19,20] thus justifying the use of a truncated form, which is illustrated in eq 4. To cover all types of bond angles present in DTMSM, the silicon-central carbon−silicon angle, methyl carbon−silicon−methyl carbon angle, and the methyl carbon−silicon-central carbon angle were studied in the above calculations.

The quantum mechanical calculations were performed using the Gaussian 98 suite of programs.[21] Both density functional theory, DFT, at the B3LYP[8] level and second-order Møller−Plesset perturbation, MP2, theory[11] were employed. Unlike other levels of theory, for example, Hartree−Fock, DFT accounts for electron correlation effects by means of the so-called exchange-correlation functional of the electron density. B3LYP stands for a Becke three-parameter nonlocal functional, B3, describing the gradient-corrected exchange energy of electrons, combined with the nonlocal functional of Lee, Yang, and Parr, LYP, which provides the gradient-corrected correlation energy of the electrons. 6-311G,[22] a triple split valence basis set assuming three sizes of contracted functions for each atomic orbital type, was used in all calculations. The selected basis set does not include diffuse or polarization functions, since the system is neutral and contains no lone pair electrons; therefore, its usage reduces the number of basis functions required to 193 only. However, a number of calculations were repeated using 6-311G* instead, and this yielded identical results in terms of energy and geometry. All electrons were included in the correlation calculations, and the zero-point energy, ZPE, was calculated in all B3LYP and MP2 calculations. Initial configurations were drawn from similar molecular mechanics, MM, calculations using a simplistic force field based on plausible assumptions about the parameter values. Physical memory equal to 15 MW was employed during the MP2(full)/6-311G calculations, while the respective amount for the ones at the B3LYP/6-311G level was reduced by a factor of 4. The CPU time ratio between the MP2 calculations and those at the B3LYP level is approximately equal to 1.35.

With regard to the output of the computations, the global minimum is characterized for both Si−CH_2 torsion angles by values of 163.6° at the MP2(full)/6-311G level and 164.4° at the B3LYP/6-311G level. Remarkably, these values coincide with the 164.0° Si−Si−Si−Si dihedral value of the minimum energy conformation of poly(dimethylsilane) reported by Sun,[13] in marked contrast with the all trans minimum energy structure of polysilane. Both of these structures were determined by means of an ab initio based force field adopting, among others, an explicit representation of hydrogen atoms. Geometry and energetics analysis had showed that the repulsion between the nearest hydrogen atoms of methyl groups attached to second neighbor Si backbone atoms highly contributes to the energy difference between the all trans and the optimized poly(dimethylsilane) helical structure. More generally, 80% of this energy difference could be attributed to Sun's[13] van der Waals interaction terms. Also, the occurrence of similar twisted

TABLE 1: Configurational Electronic Energy Difference, ΔE, of DTMSM, Relative to the Unconstrained Minimum Energy Structure, in kcal mol^{-1} (ZPE Correction to ΔE is Additionally Provided)

	level of theory			
	B3LYP/6-311G		MP2(full)/6-311G	
torsion angle	ΔE, kcal mol^{-1}	$\Delta E + \Delta$ZPE, kcal mol^{-1}	ΔE, kcal mol^{-1}	$\Delta E + \Delta$ZPE, kcal mol^{-1}
(a) Unconstrained Minimum				
164.0−164.0	0.00	0.00	0.00	0.00
(b) $CH_3-Si-CH_2-Si$ Torsion Constraints				
180.0−180.0	0.24	−0.03	0.67	0.49
180.0−150.0	0.56	0.37	0.67	0.65
180.0−120.0	1.21	0.10	1.68	1.51
180.0−90.0	0.50	0.39	0.65	0.62
150.0−150.0	1.20	1.00	1.50	1.31
150.0−120.0	2.66	2.57	3.22	3.27
150.0−90.0	2.12	1.95	2.69	2.70
120.0−120.0	3.92	3.89	4.79	4.95
120.0−90.0	2.49	2.40	3.07	3.40
90.0−90.0	1.03	0.84	1.35	1.14
(c) $CH_3-Si-CH_2-Si$ Torsions and $Si-CH_2-Si$ Bending Constraints				
−3.0	0.41	0.15	0.85	0.70
−2.0	0.31	0.05	0.75	0.59
−1.0	0.26	−0.01	0.69	0.52
+1.0	0.26	−0.02	0.69	0.50
+2.0	0.31	0.02	0.75	0.54
+3.0	0.39	0.10	0.84	0.62
(d) $CH_3-Si-CH_2-Si$ Torsions and One $CH_2-Si-CH_3$ Bending Constraints				
−3.0	0.19	0.17	0.81	0.64
−2.0	0.10	0.09	0.73	0.56
−1.0	0.03	0.03	0.69	0.51
+1.0	0.01	0.00	0.69	0.50
+2.0	0.04	0.03	0.73	0.55
+3.0	0.10	0.07	0.81	0.62
(e) $CH_3-Si-CH_2-Si$ Torsions and One $CH_3-Si-CH_3$ Bending Constraints				
−3.0	0.37	0.13	0.80	0.62
−2.0	0.30	0.05	0.73	0.54
−1.0	0.25	−0.00	0.69	0.50
+1.0	0.25	−0.03	0.69	0.50
+2.0	0.30	−0.01	0.73	0.55
+3.0	0.36	0.05	0.79	0.62

minimum energy conformations at nearly the same dihedral angle value has been confirmed by molecular simulations for poly(isobutylene).[12] Thus, our findings corroborate the importance of side groups attached to the polymer backbone, in macromolecular conformational behavior.

In an earlier experimental study of DTMSM geometry via electron diffraction,[23] an unusually wide Si−C−Si angle of 123.2° has been named as the main steric strain relieving factor, together with methyl group torsion and bond elongation. Our ab initio results show all three features to be present, for example, a Si−C−Si angle ranging from 119.3 to 124.6°, depending on the conformation examined. However, the model in that study[23] failed to identify the $Si(CH_3)_3$ moiety torsion as an important strain relaxation mechanism, which indeed is revealed by our calculations. As a consequence, one may state that spectroscopic and other experimental methods should be profitably combined with quantum mechanical and/or classical molecular mechanics calculations to produce new and improved molecular models.

Table 1 lists the energy values of all encountered configurations with respect to the global minimum structure. Their energy difference, including ZPE, is also provided in the same table. With the aid of the available conformation space points, a Ramachandran plot was constructed in Figure 2. The coordinates

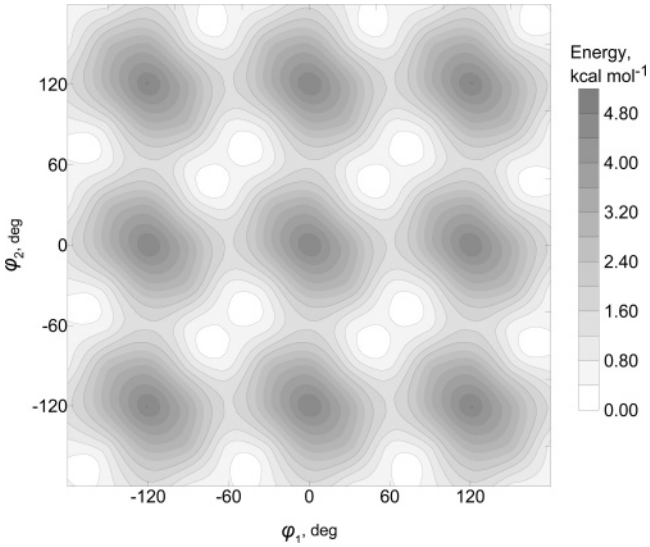

Figure 2. Ramachandran plot of the DTMSM energy landscape. The axes represent $CH_3-Si-CH_2-Si$ torsion angles in degrees, and the gray scales denote energy in kcal mol^{-1}.

in the plot correspond to the two main torsion angles, φ_1 and φ_2, and represent rotations of the two $Si-CH_2$ bonds, namely, $Si(2)-CH_2(3)$ and $CH_2(3)-Si(4)$, with reference to Figure 1. Bond lengths and bond angles, as determined by the two adopted levels of theory, were found to differ by less than 1% for all configurations. As Szalay et al.[24] have pointed out, correct reproduction of torsional energy is achieved when properly transforming the internal coordinates into symmetrized ones, thus removing any arbitrariness in the definition of dihedral angles. Taking this into account, transformed dihedral angles of the form

$$\tau_i = (\phi_{i1} + \phi_{i2} + \phi_{i3})/3 \tag{8}$$

were calculated for all given configurations in sections a and b of Table 1, where φ_{ij} denotes all possible dihedral angles which could be defined with respect to a specific rotated $Si-CH_2$ bond, i denotes any such bond, $Si(2)-CH_2(3)$ or $CH_2(3)-Si(4)$, and j denotes any of the three methyl groups attached to Si(2) or Si(4) atoms, namely, $CH_3(1)$, $CH_3(6)$, and $CH_3(7)$ or $CH_3(5)$, $CH_3(8)$, and $CH_3(9)$, respectively, as shown in Figure 1. The two values, φ and τ, were never found to differ by more than 2.0°. Given the approximations already inherent in our united atom model, inclusion of τ values would not lead to substantial improvement. Hence, for the purpose of convenience, the φ_1 and φ_2 values are used throughout our calculations, which are defined by atoms $CH_3(1)-Si(2)-CH_2(3)-Si(4)$ and $Si(2)-CH_2(3)-Si(4)-CH_3(5)$, respectively.

As one can infer from Table 1 and the aforementioned results concerning molecular geometry, the two methods employed, namely, B3LYP/6-311G and MP2(full)/6-311G, provided quite similar results. On the other hand, inclusion of ZPE in the case of the B3LYP/6-311G results inverts the order of the 164−164 and all trans conformations, attributing lower ground state energy to the latter. In detail, B3LYP/6-311G is capable of locating the global minimum, but it is the assumed harmonic oscillator correction that lessens the accuracy of the results. From this point of view, one should check the validity of the ZPE calculated correction itself and probably adopt the hindered rotor approximation for certain low-frequency modes.

III. Force Field Parametrization

As in ref 4, a fixed bond length version of the model and a fully flexible one were constructed. In the chosen representation of DTMSM, one kind of bonds and torsion angles, namely, Si−C, three kinds of bond angles, namely, Si−CH_2−Si, CH_2−Si−CH_3, and CH_3−Si−CH_3, and two kinds of local nonbonded pairs, namely, CH_2−CH_3 and CH_3−CH_3, exist. A constant, k_x, and an equilibrium value, $x°$, where x represents l or θ, are required for the quadratic stretching and bending potentials, eqs 2 and 3; one constant, namely, k_φ, fully describes the torsional term, eq 4, and a potential well depth, ϵ, and an effective cross section, σ, correspond to each of the nonbonded pairs, eq 5. Thus, there are 11 constants for the constrained and 13 constants for the flexible model to be determined. It should be noted that all 13 bond angles were considered in our calculations, whereas 11 of them suffice to provide, together with main torsion angles, bond lengths, Euler angles, and center-of-mass coordinates, the appropriate number of degrees of freedom. This is dictated by the symmetry of DTMSM, which becomes evident in its united atom representation. For example, excluding one CH_3−Si−CH_3 angle per silicon atom would lead to an unphysical symmetry breaking.

The force field development was completely based on the MP2(full)/6-311G results. It should be noted that all configuration points were characterized by vibrational analysis and ZPE corrections were included in their energy values, allowing for a proper description of the system's energy. The procedure consisted of two stages. In the first one, the atomic coordinates determined by ab initio calculations were held constant while the force field parameters varied so as to minimize the following objective function:

$$F = \frac{\sum_{i=1}^{N_{\text{conf}}} (V_i^{\text{MP2}} - V_i^{\text{FF}}(\mathbf{p};\mathbf{r}_i))^2}{\sum_{i=1}^{N_{\text{conf}}} (V_i^{\text{MP2}})^2} \qquad (9)$$

where V_i^{MP2} represents the quantum mechanical energy with respect to the fully optimized structure and V_i^{FF} the force field energy of the ith configuration, the force field parameters are collectively denoted by $\mathbf{p}$, and $\mathbf{r}_i$ refers to the quantum mechanically determined atomic coordinates of the ith configuration. In this stage, $\mathbf{p}$ comprises the independent variables, that is, the ones that are allowed to vary during the minimization procedure, while $\mathbf{r}_i$ enter parametrically and are held fixed throughout the calculation. In the second stage, the parameters obtained were evaluated by minimizing the force field energy with respect to the atomic coordinates. Once the force field constants were determined, the first stage was repeated to check the consistency of the results.

A. Fixed Bond PDMSM Model. At first, the constant bond length version of the model was constructed. Various alternative approaches were employed in an effort to locate the optimum force field parameter values. These approaches included (i) conventional direct minimization of the objective function F, eq 9, using a local search algorithm, (ii) use of equilibrium bond angles fixed at various plausible values and solving for the linear equation set occurring when the energy first partial derivatives with respect to the rest of the parameters equal zero, (iii) separate determination of bending parameters using the constrained bond angle ab initio results, (iv) optimization of all parameters except the equilibrium angles, θ_{ijk}°, which were randomly picked from a 20.0° wide interval centered at their initial values and held fixed throughout the minimization calculation, and (v) combination of approach iv with penalty functions to exclude unrealistic parameter values. The conjugate gradient optimization method was the local search algorithm selected, with numerically calculated objective function derivatives. It was realized that strategies i and iv, after screening out any unphysical results, yielded the lowest objective function values together with the most plausible results in terms of force field parameter values. The parameter sets found exhibited an enormous similarity except for their equilibrium bond angles and were rated according to their ability to reproduce the energetics with respect to the global minimum and geometrical parameters of each particular quantum mechanically calculated conformation.

In all adopted approaches throughout the parameter determination stage, the objective function, eq 9, was minimized for the given ab initio configurations. However, this procedure does not imply that molecular energetics, as ascribed by each parameter set, is itself optimum. For a complete rating of the derived model variants, single molecule energy optimization via MM calculations was performed. They included search for the minimum energy structure and constrained energy minimization calculations, where the two main torsion angles were fixed. Again, conjugate gradients with numerically computed energy derivatives were used throughout the calculations. The same value of 1.910 Å, as in the previous model version,[4] was employed for the Si−C bond length throughout those calculations.

Global Minimum. Slightly deformed all trans configurations were employed as starting geometries, and most of the model variants were able to locate a minimum energy structure bearing the quantum mechanical one. Other initial structures, like the configuration produced by the unconstrained quantum mechanical calculations, and a twisted structure with both dihedrals equal to 150.0° were also incorporated as alternative starting points. In addition, randomly chosen conformations were occasionally used to ensure convergence to the same final point.

Constrained Minima. Configurations produced by ab initio calculations, with constrained dihedral angles, were used as starting points for the minimization algorithm. However, the quantum mechanically global minimum configuration, resulting from an unconstrained optimization, was also encountered in this set of calculations with its main dihedral angles serving as the constrained ones.

To precisely express the efficiency of each model, three relevant quantities were calculated: (i) the percent error in energy reproduction, (ii) the root-mean-square error in bond angle value reproduction averaged over all constrained configurations, and (iii) the root-mean-square error in dihedral angle value reproduction per configuration, averaged over all unconstrained minimization attempts. Dihedral angles were considered separately due to their significant contribution to the complexity of macromolecule conformational behavior.

Parameter sets unable to locate the real minimum energy conformation, as predicted by ab initio calculations, have been excluded from further consideration. Moreover, these sets resulted in poor energy matching and in the poorest bond angle matching when compared to all other sets. Consideration of the above efficiency criteria combination led us to retain only two sets for further investigation, henceforth referred to as "Fix-1" and "Fix-2". Energy minimization calculations were repeated for these parameter sets, using a variety of Si−C bond lengths from 1.880 to 1.920 Å, in accordance with values either available in the literature[20,23,25] or produced by our ab initio

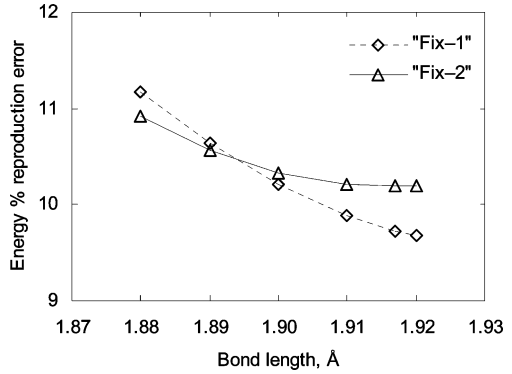

Figure 3. Percentage of energy reproduction error for the Fix-1 and Fix-2 models, with respect to preselected Si−C bond lengths.

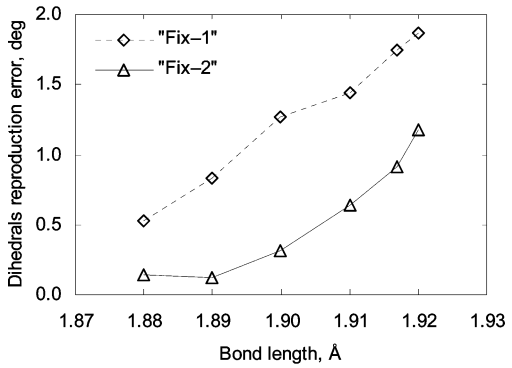

Figure 4. Dihedral angle reproduction error in deg, for the Fix-1 and Fix-2 models, with respect to preselected Si−C bond lengths.

calculations. In assessing these results, more criteria were considered, such as matching main chain bond angle values, due to their contribution to the average dimensions of the polymer molecules, and even the difference between two successive angles, which, as explained in the Introduction, accounts for the special conformational behavior of PDMSM-like molecules.

Sample results from refinement calculations are depicted in Figures 3 and 4. The energy reproduction efficiency, shown in Figure 3, is considerably improved with longer bond lengths, especially for the Fix-1 model. On the contrary, dihedral angle reproduction efficiency, Figure 4, improves with shorter bond lengths and the Fix-2 model has proven to be superior to Fix-1. In general, the results of our assessment criteria suggested the necessity for a compromise substantiated in the parameter values shown in Table 2, namely, those of the Fix-2 model. Available stretching potential parameters, which constitute the subject of the next subsection, are also given therein. The Fix-1 model parameters, if different from the adopted ones, are provided within parentheses in the same table.

B. Flexible Bond PDMSM Model. Next, we enhance the fixed bond model through further addition of a stretching quadratic potential energy term. All bonds connecting united atoms were considered to be of the same type, Si−C; therefore, one stretching constant, k_l, and one equilibrium bond length, $l°$, were calculated. Given the equilibrium bond length, ab initio configurational energies relative to the global minimum, and constant bond length force field energies, the stretching constant, k_l, was evaluated using least-squares methodology.

The percentage error of the enhanced force field energy with respect to the ab initio one was calculated for certain equilibrium bond length, $l°$, values. Only a small improvement was noticed for selected bond lengths close to the average quantum mechanical one, 1.917 Å, yielding a stretching constant equal to 986.0 kcal mol^{-1} Å^{-2}. Such a high constant would result in fast vibrations, which are difficult to follow numerically during a MD calculation without substantially reducing the time step; therefore, stretching constant values equal to 123.2, 246.5, 493.0, 739.5, and 986.0 kcal mol^{-1} Å^{-2} were tested in energy optimizations. Low improvement in energy estimation was achieved through reduction of the stretching constant, for example, force field energy percent error ranges between 9.68% for the larger test value and 9.47% for the smaller one, at the cost of an insignificant increase in deviations regarding bond lengths, bond angles, and main chain bond angles. Using low constant values, the minimum energy torsion angles were calculated within an error of less than 1.5°, while higher constants yielded inaccurate values. In all respects, low stretching constants would be preferred over higher ones. Therefore, enhancement of the fixed bond model by a quadratic stretching potential with a 1.917 Å equilibrium bond length and the lowest constant tested of 123.2 kcal mol^{-1} Å^{-2} was our selection for the fully flexible model.

The PDMSM model attributes the CH_3 united atom and CH_2−Si−CH_3 angle parameters to CH_2 and CH_2−Si−CH_2, respectively. With this assumption, the values of our polymer model are presented in Table 2. Finally, the selected set of parameters was checked for self-consistency; that is, the coordinates produced by force field energy minimization were given as input to the program optimizing the objective function, eq 9, instead of the ab initio ones, and practically the same force field constants were obtained. Stretching potential parameters are included in Table 2 together with the ones for the fixed bond models.

TABLE 2: Proposed PDMSM Force Field Local Parameters[a]

Nonbonded Terms					
Si		CH_2		CH_3	
σ, Å	ϵ, kcal mol^{-1}	σ, Å	ϵ, kcal mol^{-1}	σ, Å	ϵ, kcal mol^{-1}
2.369	0.791	3.407	0.289	3.407	0.289

Bonded Terms		
torsions		
		k_φ, kcal mol^{-1}
CH_3−Si−CH_2−Si		0.735 (0.765)
bond angles		
	k_θ, kcal mol^{-1} deg^{-2}	θ_0, deg
CH_2−Si−CH_2	0.0315	111.6 (107.7)
CH_2−Si−CH_3	0.0315	111.6 (107.7)
CH_3−Si−CH_3	0.0282	113.5 (105.1)
Si−CH_2−Si	0.0373	119.2 (116.1)
bonds		
	k_l, kcal mol^{-1} Å^{-2}	l_0, Å
Si−C	123.2	1.917

[a] All parameters, except bond stretching ones, were determined within the framework of a fixed bond length model. The parameters adopted are those of the Fix-2 model (see text for details). Fix-1 model parameters, whenever different from the Fix-2 ones, are also provided in parentheses. The proposed model, Fix-2, augmented by a stretching potential term with parameters herein shown, produced very good results in terms of energy and geometry reproduction, and, thus, constitutes the fully flexible version of our model.

IV. Force Field Validation Tests

As stated in the introductory section, our primary aim is to develop the local part of a force field with improved efficiency

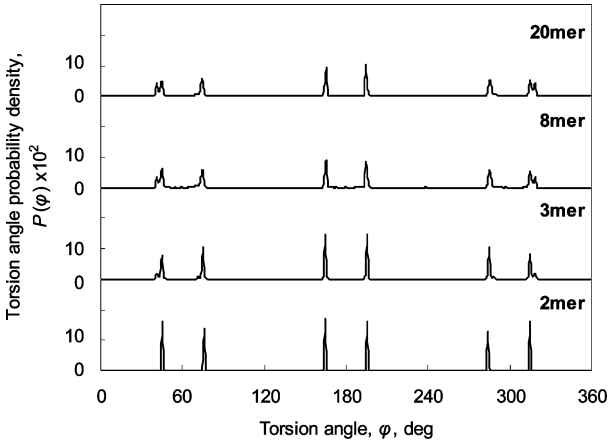

Figure 5. Torsion angle probability density, $P(\varphi) \times 10^2$, of energy optimized ideal PDMSM chains of various lengths.

in terms of the polymer conformational behavior. Our validation calculations proceed in the same direction, with an emphasis in predictions of conformational dependent properties.

A. Polymer Conformational Properties. MM energy minimization calculations were extended from DTMSM to longer PDMSM chains, namely, trimers, octamers, and eicosamers. These were subjected to local interactions only, having in mind the notion of an "ideal", "unperturbed", or "phantom" chain,[26] in which nonlocal interactions are completely absent and, therefore, the chain is allowed to cross itself at topologically distant sites. A number of randomly chosen initial conformations ranging from 300, in the case of eicosamers, up to 1200, in the case of trimers, was used in order to obtain the minimum energy dihedral angle distributions shown in Figure 5, compared with that of DTMSM, the dimer. The double minima effect is very clearly exhibited in the form of pronounced peaks on both sides of trans, as well as *gauche*±, main chain bond conformations. Another important remark is that near trans conformational states remain sharply concentrated about their average values, as the chains become longer, while near gauche states become more diffuse or less densely populated. This could probably be attributed to a "pentane effect" of the $Si-CH_2-Si-CH_2-Si$ subchains. In other words, near gauche states often lead to higher energy conformations, where two nonbonded Si atoms are brought to a very close contact.

The characteristic ratio, C_∞, is worth studying, since it represents an important aspect of the polymer's conformational behavior. Considering a linear homopolymer, C_∞ is defined as

$$C_\infty = \lim_{N\to\infty} C_N = \lim_{N\to\infty} \frac{\langle r^2\rangle_0}{Nl^2} \tag{10}$$

where r is the polymer end-to-end distance, N is the number of backbone chain bonds, and l denotes a bond's length. Therefore, the characteristic ratio is a measure of the average macromolecular size. The broken brackets denote the average over all possible polymer conformations, and the subscript "0" implies ideal or "Θ" conditions.[26] These conditions are encountered when a proper Θ solvent is used or a specific Θ temperature is attained. Under these conditions, intermolecular and nonlocal intramolecular interactions cancel out and macromolecular conformational behavior is governed by local interactions. Pure polymer melts also exhibit this kind of behavior.[27]

A polymer chain under such conditions is said to behave as an ideal chain, since only local interactions seem to contribute substantially to the macromolecule's conformational ensemble. This equivalence dictates a method of theoretically predicting the characteristic ratio by modeling the polymer in its ideal state, that is, simulating an ensemble of single isolated chains subject only to local intramolecular interactions. However, the range of local interactions need not be confined in pairs separated by three or four bonds as defined earlier. Indeed, unperturbed behavior in real systems stems from the fact that correlation between two segments belonging to the same molecule falls off exponentially as the number of bonds between them is getting larger.[28] Since there can be no sharp distinction between correlated and uncorrelated segments, one should experiment with increasing the local interaction range, n, measured in backbone chain bonds, until an asymptotic value can be determined. At the same time, n should be kept low with respect to the number of bonds, N, so that the assumption of unperturbed chains remains valid. Therefore, the prerequisites for the C_∞ value to be theoretically predicted are that the polymer model correctly incorporates the local interactions and that the following conditions hold simultaneously:

$$n \to \infty,\ N \to \infty, \text{ and } \frac{N}{n} \to \infty \tag{11}$$

The approach of gradually extending local interactions has led to the successful prediction of the poly(propylene) characteristic ratio by means of single chain Monte Carlo, MC, simulations[29] using an atomistic force field.[9] In a similar fashion, Yamakawa and Yoshizaki[30] have performed MC simulation of a freely rotating chain subject to local Lennard-Jones interactions from the fourth through nth segment. According to their conclusions, a strictly quantitative prediction of the polymer's asymptotic, $N \to \infty$, conformational behavior requires extension of n to infinity.

Our work involved single chain MC calculations for N equal to 250 with the local interaction range, n, extended from 4 to 11 bonds separating interacting sites, for N equal to 500 and n extending from 10 to 11, and also for N equal to 1000 and n equal to 15, conforming to the conditions imposed by eq 11. A truncated version of the Lennard-Jones potential was used, in which zero value was attributed beyond a cutoff radius equal to 2.5 times σ_{ij}, the pair diameter, whereas, at distances closer than a hard sphere diameter equal to $0.7\sigma_{ij}$, the energy was considered to be infinitely high. Therefore, all MC moves resulting in interacting pairs with distances closer than a hard sphere diameter were immediately rejected.

The dihedral angles are the ones that mainly affect the polymer's conformational statistics. However, the synergy of bond angles with dihedral ones is important, since it allows for the system's relaxation to low-energy configurations. Therefore, three types of MC moves were considered in our calculations: (i) rigid body rotation about a randomly selected main chain bond, (ii) rigid body "tilt" due to altering a randomly selected main chain bond angle, and (iii) reorientation of a randomly selected methyl bond while preserving its length. Using those three moves, all internal degrees of freedom considerably affecting conformational properties were taken into account. The relative frequency of move types, namely, i:ii:iii, was equal to 1:1:4. Each calculation consisted of 10^5 up to 1.2×10^6 "cycles", depending on the chain length and convergence rate, with 100 MC moves executed per cycle. A straight conformation was the starting point for each calculation. The chain was "crumpled", and the energy running average was monitored until reaching an equilibrium value. Then, the chain configuration was recorded and average values were computed at the end of each cycle.

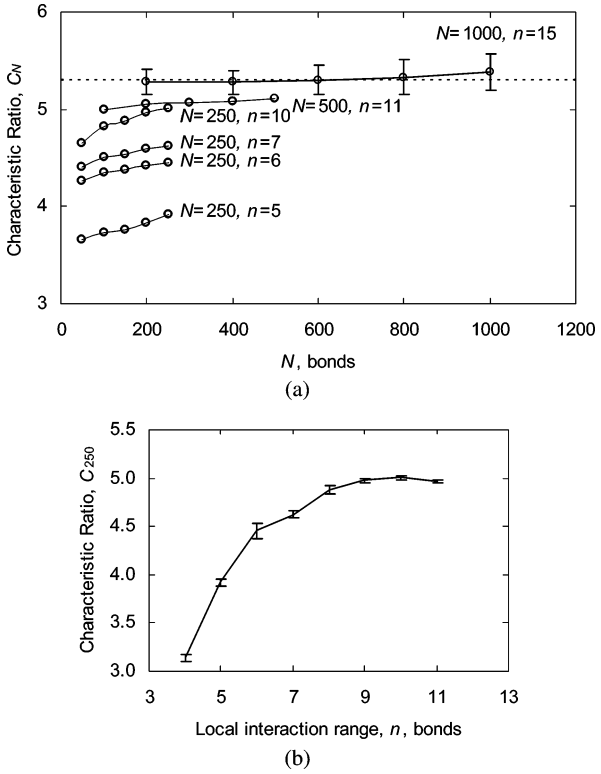

Figure 6. (a) Characteristic ratio, C_N, with respect to the local interaction maximum range, n, and polymer chain length, N, both measured in main chain bonds. The dotted line represents the available experimental value. (b) Characteristic ratio, C_{250}, with respect to the local interaction maximum range, n, measured in main chain bonds. In both cases, error bars are attributed by block averaging.

The temperature in all runs was set to 300.00 K. The characteristic ratio of the simulated chain and its subchains were calculated, considering all long enough parts of each chain to be unperturbed. Our results are depicted in Figure 6, and a characteristic ratio value of 5.4 ± 0.2 is attained toward the asymptotic limit, comparing remarkably well to 5.3, the experimental value of Mark and Ko.[31]

B. Dimer Structural, Thermodynamic, and Transport Properties. Further evaluation of our revised model included five MD runs for a system of DTMSM molecules. The simulated system consisted of 81 DTMSM molecules subjected to cubic periodic boundary conditions. The initial box length was equal to 30.542 Å, corresponding to a density of 0.757 g/cm^3, very close to the experimental one at 298.15 K.[32] All MD runs were performed in the isothermal−isobaric, *NPT*, ensemble at atmospheric pressure and temperatures equal to 273.15, 293.15, 298.15, and 333.15 K, to compare with available experimental density values,[32] and also equal to 300.00 K, conforming to ref 4. The system was simulated for a period of 6 ns. The first 1 ns interval was considered as the equilibration stage and was not considered in our results. Nonlocal parameters and other simulation details were the same as those in ref 4.

The dihedral angle distribution was calculated for the MD trajectories. This distribution is shaped by the synergy of all forces acting on each interaction site, namely, stretching, bending, torsional, and nonbonded. On the basis of this distribution, an effective torsional potential was determined and compared to a simplistic sinusoidal fitted representation. Namely, the probability density, $P(\varphi)$, of locating a dihedral angle in the range φ and $\varphi + \Delta\varphi$ implicitly defines the effective potential, $V_{\text{eff}}(\varphi)$, by means of

$$P(\phi) = \frac{e^{-V_{\text{eff}}(\phi)/k_B T}}{\sum_{\phi} e^{-V_{\text{eff}}(\phi)/k_B T}} \tag{12}$$

where k_B denotes Boltzmann's constant and T is the absolute temperature. The resulting curve was fitted and checked against a potential of the form

$$V'(\phi) = \frac{1}{2}k_\phi(1 + \cos 3\phi) \tag{13}$$

with an appropriate constant, k_φ. A portion of the effective potential in a range of ±16.0° on both sides of the supposed trans minima is excluded from the fitting procedure. This way, deviations off the sinusoidal curve were revealed. If the effective potential were perfectly sinusoidal, it would match the respective curve in the excluded range as well as outside. This is not the case, as Figure 7 clearly shows. The effective potential is indeed seen to deviate from the sinusoidal one in the vicinity of the minima by an amount of about 0.15 kcal mol^{-1}.

This way, the existence of a remarkably flat potential energy "valley" is revealed, extended on both sides of the trans conformation. The "flatness" of this topology is mainly due to the dislocated global minima, which allows the system to explore more extended regions of the configuration space around the trans conformation. Regarding Figure 7a, the absence of two clearly distinct peaks due to the global energy minima should be attributed to a lower energy intervening saddle point provided by our force field, as compared to the quantum mechanical

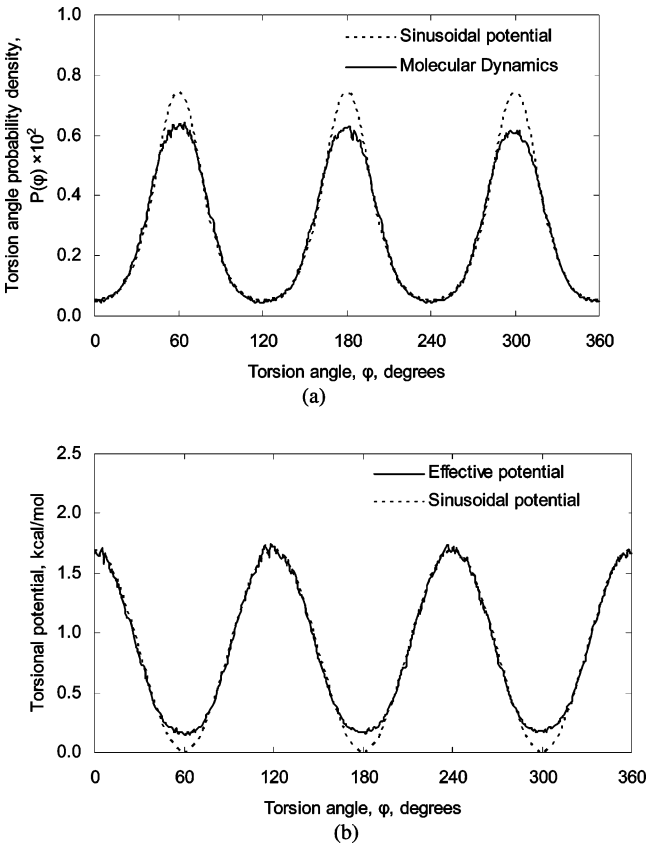

Figure 7. (a) Torsion angle probability density, $P(\varphi)$ ($\times 10^2$), of liquid DTMSM at 293.15 K and atmospheric pressure, obtained from MD simulation employing the Fix-2 model, as compared to the probability density due to a sinusoidal potential. (b) Effective torsion potential corresponding to the above torsion angle distribution, as compared to a sinusoidal potential.

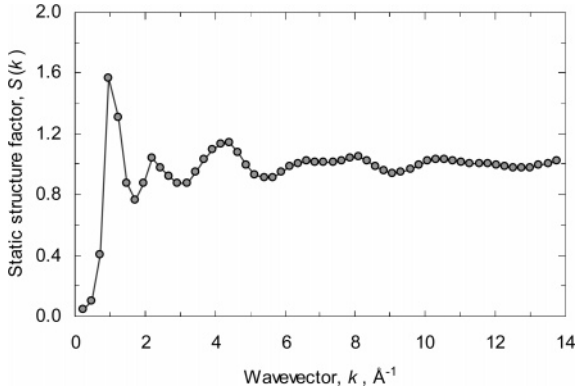

Figure 8. Static structure factor, $S(k)$, of liquid DTMSM simulated at 300.00 K and atmospheric pressure.

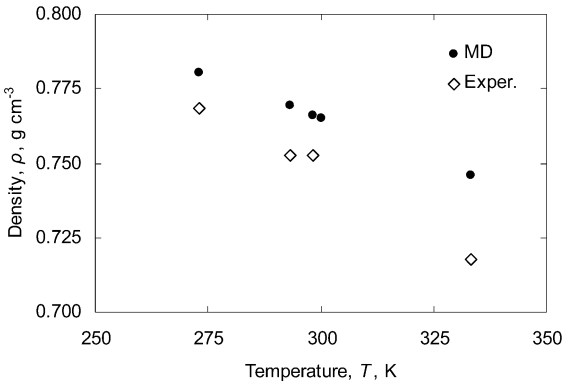

Figure 9. Calculated and experimental liquid DTMSM density values at various temperatures and atmospheric pressure.

results. Apparently, this is a limitation of the united atom representation, since the helical minimum energy conformation adopted by molecules similar to PDMSM, such as poly(isobutylene)[12] and poly(dimethylsilane),[13] has been mainly attributed to the repulsion between hydrogen atoms belonging to the side methyl groups. Nevertheless, even such a coarse grained representation is proved capable to predict peculiarities arising from side group interactions.

The static structure factor, $S(k)$, provides an indication on whether the simulated systems are realistic. $S(k)$ can be defined as

$$S(k) = 1 + \frac{\left\langle \frac{1}{V} \right\rangle \sum_{\alpha} \sum_{\beta} N_\alpha N_\beta f^\alpha(k) f^\beta(k) \int [g^{\alpha\beta}(r) - 1] e^{-i\mathbf{k}\cdot\mathbf{r}} \, d^3r}{\sum_{\alpha} N_\alpha [f^\alpha(r)]^2} \quad (14)$$

where $\mathbf{k}$ is the wavevector, V is the system's volume, α and β denote atom types, Si, CH_2, or CH_3, N_α is the number of α type atoms in the system, $f^\alpha(k)$ are analytical approximations of the respective atomic scattering factors,[33] and $g^\alpha\beta(r)$ is the radial distribution function of β type atoms around an a type one. Calculated $S(k)$ at 300.00 K is presented in Figure 8.

Limited experimental data exist regarding dimer thermodynamic and transport properties, thus reducing the number of further possible validation tests. Calculated average densities and experimental values at various temperatures are shown in Figure 9. The mean square error was 2.6%. Remarkably, the average density resulting from the NPT run at 293.15 K was 0.769 g cm^{-3}, which equals the value produced by the model used in ref 4. This justifies the distinction between the local and nonlocal parts of the force field, since our revision of the local part does not seem to affect the nonlocal dependent density, at least in the case of a low-molecular-weight oligomer, such as DTMSM.

The constant pressure specific heat, C_P, relates to fluctuations in H, the system's total molecular energy,[34] according to

$$\langle \delta(H + PV)^2 \rangle = k_B T^2 C_P \quad (15)$$

where P is the imposed pressure. Our MD data result in C_P values of 65.86 ± 5.23 cal mol^{-1} K^{-1} at 298.15 K and 74.36 ± 12.82 cal mol^{-1} K^{-1} at 300.00 K, which are lower than the sole reported value of 85.44 cal mol^{-1} K^{-1} at 298.15 K.[35]

For the sake of comparison with future experimental and/or simulation studies, additional results are also provided, based on the 300.00 K MD calculations. The cohesive energy, E_{coh}, was calculated by subtracting the total molecular potential energy out of intramolecular interactions[36] and averaging over all recorded configurations. The cohesive energy density or square of Hildebrandt's δ

$$\delta^2 = \langle E_{coh}/V \rangle \quad (16)$$

was then determined to be equal to 68.8 ± 0.1 cal cm^{-3}. The isothermal compressibility, β_T, relates to volume fluctuations[34] according to

$$\langle \delta V^2 \rangle = \langle V \rangle k_B T \beta_T \quad (17)$$

resulting in a value equal to (1.0 ± 0.6) × 10^{-3} MPa^{-1}. The self-diffusion coefficient, D_s, was determined via the well-known Einstein relation:

$$D_s = \lim_{t\to\infty} \frac{1}{6t} \langle |\mathbf{R}_i(t_0 + t) - \mathbf{R}_i(t_0)|^2 \rangle_{i,t_0} \quad (18)$$

where $\mathbf{R}_i(t)$ is the position vector for the center of mass of molecule i and $\langle \, \rangle_{i,t_0}$ denote averaging over all molecules and all time origins, t_0, of each time interval, t. The value calculated with eq 18 equals (5.6 ± 0.9) × 10^{-6} cm^2 s^{-1}. Error bars related to the quantities determined via eqs 15−18 were attributed by dividing the simulation's 5 ns production stage in five 1 ns blocks and averaging.

V. Conclusions

The DFT, namely, B3LYP/6-311G, level of theory provides high accuracy at a moderate cost in CPU time, disk space, and physical memory as compared with the perturbation theory, namely, MP2(full)/6-311G, or configuration interaction methods of similar accuracy. In this study, the two methods, B3LYP/6-311G and MP2(full)/6-311G, yielded nearly identical outputs in terms of minimum energy configuration, constrained structures, and change in energy with varying geometry. Errors inherent in the approximations used when calculating ZPE must be taken into account, to correctly compare the two methods. It is thus confirmed that B3LYP/6-311G is a powerful method, capable of providing competitive results to those of purely ab initio methods, for ground state calculations of polyatomic molecules.

To compress the information content of highly complex potential hypersurfaces of polyatomic molecules in a simple "diagonal" united atom model is, in the general case, impossible. However, by carefully tuning the available parameters, even such simple models become capable of grasping essential

features of the potential energy surface, which should be allowed to "survive" in the course of large size-scale and time-scale molecular simulation computations. In this study, we have managed to devise such a model for poly(dimethylsilylene-methylene), PDMSM, which has proven through subsequent single molecule MM and MC calculations to effectively describe the polymer conformational behavior. Bulk system MD runs were also performed in order to predict a number of important dimer properties.

Future steps of our research include (i) extension of the force field to encompass PDMSTM via quantum mechanical calculations for the respective monomer, trimethylpropylsilane, and application to the PDMSTM and PDMSM-*co*-PDMSTM simulations and (ii) derivation of a similar model for the above compounds, explicitly representing the hydrogen atoms and capable of accurately reproducing the minimum helical structure energetics.

References and Notes

(1) Clarson, S. J., Anthony Semlyen, J., Eds. *Siloxane Polymers*; PTR Prentice Hall: Englewood Cliffs, NJ, 1993.

(2) (a) Schultz, J.; Peinemann, K.-V. *J. Membr. Sci.* **1996**, *110*, 37. (b) Baker, R. W. *Ind. Eng. Chem. Res.* **2002**, *41*, 1393.

(3) (a) Rudoi, V. M.; Ogarev, V. A. *Kolloidn. Zh.* **1978**, *40*, 270. (b) Finkel'shtein, E. Sh. *Polym. Sci., Ser. B* **1995**, *37*, 185.

(4) Raptis, V. E.; Economou, I. G.; Theodorou, D. N.; Petrou, J.; Petropoulos, J. H. *Macromolecules* **2004**, *37*, 1102.

(5) Alentiev, A.; Economou, I. G.; Finkelshtein, E.; Petrou, J.; Raptis, V. E.; Sanopoulou, M.; Soloviev, S.; Ushakov, N.; Yampolskii, Y. *Polymer* **2004**, *45*, 6933.

(6) Economou, I. G.; Raptis, V. E.; Melissas, V. S.; Theodorou, D. N.; Petrou, J.; Petropoulos, J. H. *Fluid Phase Equilib.* **2005**, *228*−229, 15.

(7) Makrodimitri, Z. A.; Raptis, V. E.; Economou, I. G. *J. Phys. Chem. B*, in press.

(8) (a) Becke, A. D. *Phys. Rev. A* **1988**, *38*, 3098. (b) Becke, A. D. *J. Chem. Phys.* **1993**, *98*, 5648. (c) Lee, C.; Yang, W.; Parr, R. *Phys. Rev. A* **1988**, *37*, 785.

(9) Antoniadis, S. J.; Samara, C. T.; Theodorou D. N. *Macromolecules* **1998**, *31*, 7944.

(10) Widmann, A. H.; Laso, M.; Suter, U. W. *J. Chem. Phys.* **1995**, *102*, 5761.

(11) Møller, C.; Plesset, M. S. *Phys. Rev.* **1934**, *46*, 618.

(12) Karatasos, K.; Saija, F.; Ryckaert, J.-P. *Physica B* **2001**, *301*, 119.

(13) Sun, H. *Macromolecules* **1995**, *28*, 701.

(14) Sok, R. M.; Berendsen, H. J. C.; Van Gunsteren, W. F. *J. Chem. Phys.* **1992**, *96*, 4699.

(15) (a) Maple, J. R.; Hwang, M.-J.; Stockfish, T. P.; Dinur, U.; Waldman, M.; Ewig, C.; Hagler, A. T. *J. Comput. Chem.* **1994**, *15*, 162. (b) Hwang, M.-J.; Stockfish, T. P.; Hagler, A. T. *J. Am. Chem. Soc.* **1994**, *116*, 2515.

(16) Hagler, A. T.; Ewig, C. S. *Comput. Phys. Commun.* **1994**, *84*, 131.

(17) Smith, G. D.; Bharadwaj, K. *J. Phys. Chem. B* **1999**, *103*, 3570.

(18) (a) Smith, G. D.; Jaffe, R. L.; Yoon, D. Y. *J. Phys. Chem.* **1993**, *97*, 12752. (b) Smith, G. D.; Paul, W. *J. Phys. Chem. A* **1998**, *102*, 1200. (c) Smith, G. D.; Borodin, O.; Bedrov, D. *J. Phys. Chem. A* **1998**, *102*, 10318. (d) Smith, J. S.; Borodin, O.; Smith, G. D. *J. Phys. Chem. B* **2004**, *108*, 20340.

(19) (a) Wollrab, J. E. *Rotational Spectra and Molecular Structure*; Academic Press: New York, 1967. (b) Kroto, H. W. *Molecular Rotation Spectra*; John Wiley & Sons: London, 1975.

(20) Kilb, R. W.; Pierce, L. *J. Chem. Phys.* **1957**, *27*, 108.

(21) Frisch, M. J.; Trucks, G. W.; Schlegel, H. B.; Scuseria, G. E.; Robb, M. A.; Cheeseman, J. R.; Zakrzewski, V. G.; Montgomery, J. A., Jr.; Stratmann, R. E.; Burat, J. C.; Dapprich, S.; Millam, J. M.; Daniels, A. M.; Cammi. R.; Mennucci, B.; Pomelli, C.; Adamo, C.; Clifford, S.; Ochterski, J.; Petersson, G. A.; Ayala, J. Y.; Cui, Q.; Morokuma, K.; Malik, D. K.; Raduck, A. D.; Raghavachari, K.; Foresman, J. B.; Cioslowski, J.; Ortiz, J. V.; Stefanov, B. B.; Liu, G.; Liashenko, A.; Piskorz, P.; Komaromi, I.; Comperts, R.; Martin, R. L.; Fox, D. J.; Keith, T.; Al-Laham, M. A.; Peng, C. Y.; Nanayakkara, A.; Gonzalez, C.; Challacombe, M.; Gill, P. M. W.; Johnson, B.; Chen, A.; Wong, M. W.; Andres, J. L.; Gonzalez, C.; Head-Gordon, M.; Replogle, E. S.; Pople, J. A. *Gaussian 98*, revision A.1; Gaussian Inc.: Pittsburgh, PA, 1998.

(22) (a) McLean, A. D.; Chandler, G. S. *J. Chem. Phys.* **1980**, *72*, 5639. (b) Krishnan, R.; Binkley, J. S.; Seeger, R.; Pople, J. A. *J. Chem. Phys.* **1980**, *72*, 650.

(23) Fjeldberg, T.; Seip, R.; Lappert, M. F.; Thorne, A. J. *J. Mol. Struct.* **1983**, *99*, 295.

(24) Szalay, V.; Császár, A. G.; Senent, M. L. *J. Chem. Phys.* **2002**, *117*, 6489.

(25) (a) Lide, D. R.; Coles, D. K. *Phys. Rev.* **1950**, *80*, 911. (b) Kivelson, D. *J. Chem. Phys.* **1954**, *22*, 1733. (c) *Tables of interatomic distances and configurations in molecules and ions. Supplement 1956*−1959; The Chemical Society: London, 1965.

(26) (a) Flory, P. J. *Statistical Mechanics of Chain Molecules*; Interscience Pub.: New York, 1974. (b) Gedde, U. *Polymer Physics*, 1st ed.; Chapman & Hall: London, 1995. (c) Strobl, G. *The Physics of Polymers*; Springer-Verlag: New York, 1997.

(27) Cotton, J. P.; Decker, D.; Benoit, H.; Farnoux, B.; Higgins, J.; Jannink, G.; Ober, R.; Picot, C.; des Cloizeaux, J. *Macromolecules* **1974**, *7*, 863.

(28) Doi, M. *Introduction to Polymer Physics*; Clarendon Press: Oxford, U.K., 1996.

(29) (a) Samara, C. T. Ph.D. Thesis, University of Patras, Greece, 2001. (b) Theodorou, D. N. Variable Connectivity Monte Carlo Algorithms for the Atomistic Simulation of Long-Chain Polymer Systems. In *Bridging Time Scales: Molecular Simulations for the Next Decade*; Nielaba, P., Mareschal, M., Cicotti, C., Eds.; Springer-Verlag: Berlin, 2002; pp 69−128.

(30) Yamakawa, H.; Yoshizaki, T. *J. Chem. Phys.* **2003**, *118*, 2911.

(31) Ko, J. H.; Mark, J. E. *Macromolecules* **1975**, *8*, 869.

(32) (a) Sommer, L. H.; Mitch, F. A.; Goldberg, G. M. *J. Am. Chem. Soc.* **1949**, *71*, 2750. (b) Merker, R. L.; Scott, M. J. *J. Am. Chem. Soc.* **1963**, *85*, 2242. (c) Brady, J. E.; Herter, C. D.; Carr, P. W. *Anal. Chem.* **1984**, *56*, 278. (d) Holroyd, R.; Itoh, K.; Nishikawa, M. *Nucl. Instrum. Methods Phys. Res., Sect. A* **1997**, *390*, 233.

(33) (a) Narten, A. H. *J. Chem. Phys.* **1979**, *70*, 299. (b) Iber, J. A., Hamilton, W. C., Eds. *International Tables for X-ray Crystallography*; Kluwer Academic Publishers: 1989; Vol. IV.

(34) (a) Hill, T. L. *Statistical Mechanics*; McGraw-Hill Inc.: New York, 1956. (b) Allen, M. P.; Tildesley, D. J. *Computer Simulation of Liquids*; Oxford Science Publications: Oxford, U.K., 1987.

(35) Guseinov, Z. A.; Karasharli, K. A.; Dzhafarov, O. I.; Nurullaev, G. G.; Nametkin, N. S.; Gusel'nikov, L. E.; Volnina, F. A.; Burdasov, E. N.; Vdovin, V. M. *Dokl. Akad. Nauk SSSR* **1975**, *222*, 1369.

(36) van Krevelen, D. W. *Properties of Polymers*, 3rd ed.; Elsevier: Amsterdam, The Netherlands, 1990.